REQ. NO. 0-9169

TECHNO SCIENTIFIC INC.
3984 Cheeswood Drive, Downsview, Ontario M3J 2W6 (416)635-7626, Telex 06-986766 TOR

CONTRACT REPORT NO. OSR81-00021

Ultrasonic Monitoring of Crack Extension by Corrosion Fatigue in Oil Pipelines

FINAL REPORT on Contract

No. 23440-0-9169

to CANMET

Final Report

OCT 27 1982
MICROMEDIA

Feb. 1982

Prepared by
Dr. M. Macecek

49pp

OCT 27 1982
MICROMEDIA
Produced by
Dr. M. Hacker

TABLE OF CONTENTS

		Page
	Executive Summary	
1.	INTRODUCTION	1
	1.1 Background	2
	1.2 Principle of the Method	3
2.	EXPERIMENTAL	4
	2.1 Mechanical Design	4
	2.2 Test Pipes	6
	2.3 Pressure Cycling Equipment	6
	2.4 Corrosion Fatigue Tests	8
3.	RESULTS	10
	3.1 Crack Depth Measurements	10
	3.2 Fractography	11
	3.3 Metallography	12
4.	DISCUSSION	13
	4.1 Performance of UT System	13
	4.2 Comparison of Predicted and Observed Fatigue Lives ...	15
	4.3 Crack Initiation Uncertainty	16
	4.4 Critical Crack Length for Rupture	17
5.	CONCLUSIONS	18
6.	ACKNOWLEDGEMENTS	18
7.	REFERENCES	20
8.	TABLES	
9.	FIGURES 1 - 21	
10.	APPENDICES: A - D	
	A. H_2S Concentrations for Tests I, II, III	
	B. Pressure Spectrum During One Test Block	
	C. Temperature Variations During Tests	
	D. Fatigue Life Prediction, Based on Growth Rate of Weld Toe Defect	

Executive Summary:

The project described in this report deals with the ultrasonic monitoring of crack extension by corrosion fatigue in oil pipelines. The project is a part of a large program initiated by CANMET-EMR. The overall objective is to determine the initial acceptable defect sizes for representative operational conditions. The above project includes the study of the pressure spectrum, effect of crack orientation, effect of hydrogen sulfide content, fracture mechanics calculations of corrosion fatigue lives, and verification of predicted corrosion fatigue lives by field experiments using artificial weld toe defects.

This report describes the full-scale field experiments performed to test the fatigue lives as predicted by the laboratory work at CANMET-EMR. The ultrasonic dynamic time of flight method was used to measure the depth of cracks. An automated, computer controlled system gives near real time results and graphically displays crack profiles to an accuracy of 0.5 mm (0.020").

Three full scale pipe sections were tested. The measured fatigue lives were shorter than those predicted by FM model. The critical crack length leading to a leak or a rupture of the pipes was also established. The crack morphology was verified by fractography and metallography. Data generated from the tests were used to define the allowable crack depth for the remaining life of the pipeline.

ULTRASONIC MONITORING OF CRACK EXTENSION BY CORROSION FATIGUE IN OIL PIPELINES

1. INTRODUCTION

After only five to nine years of operation, a major crude oil transmission pipeline experienced five service failures. All of these failures resulted from initial crack-like defects located at the toe of the longitudinal pipe weld.[1]

A CANMET-EMR program was launched to determine the acceptable initial defect sizes for representative operational conditions. The study[2] consists of four parts:

1. Analysis of pressure records and development of characteristic pressure spectrum in a pipeline.
2. Analysis of effects of crack orientation, configuration, and hydrogen sulphide content in crude oil on fatigue crack growth rate.
3. Fracture mechanics calculations of corrosion fatigue lives.
4. Verification of calculated fatigue lives by full-scale field experiments, with artificial weld toe defects.

Techno Scientific Inc. (TSI) was awarded the contract by CANMET-EMR to monitor the crack growth by corrosion fatigue in a

line pipe, pressurized by a pipeline pressure spectrum. This report describes the test results of full scale pipes pressurized with a pressure cycling facility, designed and supplied by Interprovincial Pipe Line (IPL). The method, its application in tests of three capped pipe sections, and the results are described.

1.1 BACKGROUND AND OBJECTIVES

The original intent of the experiments was to monitor the growth of a corrosion fatigue crack[3] in the oil line pipe and to verify the predicted fatigue lives. The author previously developed the ultrasonic monitoring system to measure the crack depth to an accuracy of 0.5 mm (DSS contract 1SQ79-00181).

The additional objective was to determine the minimum crack length leading to a rupture of the line. The rupture versus leak relationship is of importance to the utility (IPL), since NDE method to be used for in service inspection of the oil pipeline detects only long cracks. The short, undetected cracks should result in leaks only.

1.2 PRINCIPLES OF THE METHOD

The ultrasonic method devised to monitor crack depth is based on the dynamic time of flight method (Figure 1). A highly focused transducer with a long focal length is moved along the circumference of the pipe in the close vicinity of the longitudinal weld.

In the absence of the crack an electronic reference level is used to mark the inner wall of the pipe. As the transducer moves closer to the weld, the oblique beam intercepts the crack starting with the corner reflections, which give the longest time of flight, and the beam is progressively reflected from higher and higher points on the crack until the crack tip is reached.

To determine the time travel versus distance dependence, a scan is performed. This scan is perpendicular to the weld axis while maintaining the orientation and distance to the pipe of a transducer.

The shortest travel time corresponds to a crack tip. The depth of a crack from the reference level can be then calculated with the help of a simple formulae. A special system was developed to deal with the weld geometry. The system is mechanically rigid:

the UT head follows the curvature of the pipe, and immersion coupling fluid assures the transfer of UT energy.

The crack monitoring method is a simplified version of the technique used by the author elsewhere [4], using only one transducer. A fully computerized near real time system is used to evaluate the pipe flaws after calibration. This system uses a Z-80 microcomputer and the software is done in machine language. The block diagram is shown in Figure 2.

2. EXPERIMENTAL

2.1 MECHANICAL DESIGN

A 10 foot long standard "Gullco" welding track (Aluminum Alloy) complete with a centre drive gear rack is strapped to the pipe section. An aluminum travel carriage runs on the track via adjustable heavy duty ball-bearing wheel assemblies. The carriage is driven by a stepping motor which transfers its power to the system through a drive gear, timing belt and timing pulley

system. All power connections and ultrasonic connectors are mounted on the main body of the carriage.

Adjustable aluminum arms pivoted on the carriage body hold and adjust the 22.5 cm (9") long band segment rolled to conform to the curvature of the test pipe. The band segment is held to the test section by electromagnets which are activated during each circumferential scan (X-axis). The magnets are switched off when the carriage moves parallel to the weld (Y-axis). Ten 1.2 cm (1/2") long spacers hold the band at a constant distance from the pipe surface. The ultrasonic transducer head is rigidly held by a second band system which moves on the fixed band segment by means of four teflon sliders. A linear actuator moves the UT system on the X-axis in steps of 0.05 mm (0.002"). The overall view of the system mounted on the test pipe can be seen in Figures 3 and 4.

During testing the calibration consisted of adjusting the electronic reference level in such a way that the results obtained matched the true depth of calibration notch within 0.2 mm. When the results on preliminary calibration holes were accurate to 0.025 mm, the system was considered calibrated and ready for field use. However, the variations in the pipe and the weld geometry necessitated the use of a shallow calibration notch

directly on the pipe section being tested. The calibration notch was made considerably shallower than the test grooves, thereby guarding against any growth of the calibration notch.

2.2 TEST PIPES

Three test sections, 2.4 - 3.5 m long, 7.5 mm wall thickness, 914 mm (36") diameter, were made from the pipe dug out of the existing IPL line (ERW welded over by SAW). The initial notches detailed in Table I and Figure 5 were cut at the toe of the longitudinal weld. The width of the notch, was about 0.25 mm (0.010"), was governed by the size of the slotting saw (the Cleveland Twist & Drill Co., jewelers' slotting saw 0.2 mm (0.008") wide). The cutting machine (designed at the University of Waterloo) vibrated somewhat, hindering the notch cutting. Two end caps containing the nozzles, nipples, valves, and a pressure gauge were welded on by IPL Westover Yard personnel. After the girth welds were X-rayed, the vessel was delivered to the test site and connected to the pressure cycling facility.

2.3 PRESSURE CYCLING FACILITY

The facility designed and assembled by IPL [5] was capable both

of cycling a fluid filled test section of pipe through a random pressure sequence and of reaching the burst pressure of 20,680 kPa (3,000 psi). A single acting duplex pump, with maximum flow rate of 6.7 US GPM, powered the system. Crude oil with $\sim$ 100ppm of H_2S content was used as the testing medium.

The H_2S was dissolved into the oil by bubbling the gas through the sump tank. The escaping H_2S was neutralized by a NaOH bath, so no health hazard was created. However, the operator used a Scott-Airpack breathing apparatus during the procedure. The desired level of H_2S was 100 $\pm$ 50 ppm. The concentration of H_2S was measured by Standard Biological Laboratories, Mississauga, using the Potentiometric Titration of Hydrogen Sulfide (UOP Method 163-59). Samples were taken from the test section outlet using the 25 ml glass containers closed with a teflon seal. The chemical analysis gave the H_2S concentration to $\pm$ 20 ppm The H_2S level was first raised to about 180-200 ppm (verified by one sample analysis). The level was then left to stabilize. After 24-48 hours the concentration dropped to 130-150 ppm due mostly to the absorption of H_2S by the metal pipe section. The concentration then remained steady with continuous decline, and was again monitored. The H_2S data for tests I, II and III are given in Appendix A.

The representative pressure spectrum block shown in Appendix B was derived by Canmet-EMR based on the charts from a pumping station [6]. Each test block was performed in a span of 30-50 minutes.

2.4 CORROSION FATIGUE TEST

Three pipe sections were tested. The first pipe, which was tested in fine early fall weather, leaked after only 106 blocks. The fatigue life was shorter than that predicted by the theoretical model. Shallower notches were then cut in the next pipe section for the second test. This resulted in an enormous extension of test time, to 1009 blocks, which is equivalent to 84 years of operation. The third test was the shortest (82 blocks).

Because of its complexity, the entire system was prone to failure. We experienced the failure of the control valves and of the analog computer; the pump seals began to leak and a crack appeared in the nipple on the pressure vessel; and the mechanics of the magnetic floppy disk drives of the digital computer gave us considerable trouble in cold weather. We eventually overcame all these problems and carried out regular testing.

The monitoring of crack depth was to occur at intervals of 0.5 mm crack extention, but this goal proved overly-optimistic. The scatter in growth rate, the variations in original notch depths produced by machining, the availability of the pumping system, and finally the weather, all governed the intervals between measurements.

As days grew colder, the ultrasonic equipment exhibited a considerable drifting of parameters (namely gate width and position) when it was turned on. Leaving the equipment on permanently minimized this drifting.

In November and December the weather became so harsh that the coupling fluid froze in the feeder tube. IPL kindly responded by erecting a tent-like structure above the pressure vessel for the third test. The change improved conditions for both the ultrasonic scanner and the operators.

The outside temperature was also monitored. The oil stayed at about 5^{o} C above the ambience, but its viscosity sometimes was high enough (waxing phenomenon) to cause a shutdown of the system. The temperature values appear in Appendix C.

To take measurements, it was necessary to shut down the pumping system. Ultrasonic measurements were made at lower pressures

(300 psi). The ultrasonic scanner with a supply of coupling fluid was remounted on the pipe section and the calibration notch, was measured first, followed by the actual measurement of the cracks. The results were displayed on the CRT screen and then printed on a hard copy printer.

3. RESULTS

3.1 CRACK DEPTH MEASUREMENTS

The list of original notches is displayed in Table I and the typical layout of the notches shown in Figure 5. Base line inspection was carried out before H_2S was introduced.

The interim inspections were performed with the standard axial steps of 6.25 mm (0.25"); occasionally a finer step of 3.12 mm (0.125") was used. The step was software selectable. The results in terms of crack depth versus number of blocks are shown in Figures 7 and 8 and tabulated in Table II. Figure 6 shows the change in one crack profile during the test.

3.2 FRACTOGRAPHY

The ultrasonic results were verified by both fractography and metallography.

The areas of the cracks where leakage occurred were cut out, cooled in liquid nitrogen, and then broken. The freeze-break fracture faces of failures in the first two tests are shown in Figure 9.

The leaks on the pipe were not visible to the naked eye, although the failure of the vessel in test no. 1 resulted in an oil jet about 6 metres high. The leak in test no. 2 was much smaller and resulted in approximately 90 litres (twenty gallons) of oil being pumped out into the pond. This leak was not large enough to cause the computer to shut down the system, so the shutdown occurred only when the auxiliary tank was drained. Figure 10 shows the oil jet rising from the pipe section, under a pressure of $\sim$ 200 psi.

Test no. 3 resulted in a violent rupture that bent and destroyed the scanning apparatus drive. The resulting opening was 1 metre long and caused an immediate shutdown of the pressure cycling facility. Figure 11 shows the appearance of the vessel after the rupture and Figure 12 is an illustration of the fracture after it

was cut from the pipe. Figure 13 shows the edge of the original notch, the fatigue crack, and the final ductile fracture.

One feature of the fracture surface faces common to all three tests is the faceted morphology of the surface. In Figure 9, the faceted surface looks like a concrete block wall. It is interesting to note that this phenomenon, so apparent in our own testing and the field failure, was observed to a lesser degree in the laboratory experiments of EMR; apparently the steel used in laboratory experiments was cleaner. Ultrasonic scanning made it possible to detect the facets along crack surfaces and will be discussed later.

3.3 METALLOGRAPHY

Most of the metallography was done at WIC by J.M. Irvine. The objective was threefold: to verify the original notch depth, to verify the crack depth values, and to study the morphology of cracks. The series of figures from 14 to 18 shows the typical notch shape, its position with reference to the root pass of the weld, and whether the cracks are shallow, deep, or multiple. In all cases the cracks were initiated from the notches. The shapes of the cracks indicate that they are:

- very tight
- either branched or stepped
- vary in direction from 70^{o} to 110^{o} to the plate surface.

4. DISCUSSION

The experiments generated a wealth of knowledge, specifically in three main areas:

- real time ultrasonic monitoring of crack growth
- corrosion fatigue lives under spectrum loads
- leak versus rupture mode of failure of the line.

4.1 PERFORMANCE OF THE UT SYSTEM

The real time ultrasonic monitoring performed well even under adverse ambient conditions, consistently producing a high signal to noise ratio (S/N). The immersion coupling was likely responsible for the stability of the signal. The deposition of a thin layer of industrial grease decreased the friction of the scanning head, minimized the leakage of couplant, and limited the wear of the coupling shoe. Later in the program, cold weather was responsible for the drifting of the gate and other parameters of the UT system. These problems were resolved by leaving the

system "on" and adding space heaters to the control trailer.

Test pipe no. 2 presented yet another problem. The weld geometry here was irregular (weld wander), requiring the correction of the circumferential start position. The weld wander was also responsible for the less than ideal position of the original notch, slightly away from the weld toe (see Fig. 18).

The morphology of the cracks, as shown in Figures 14-18, indicates that corrosion fatigue cracks are very tight. Although there have been some doubts that a sufficient signal will be received from areas close to the tip of the crack, our experience proves that, for the transducer used, a very good UT response was obtained. We have no evidence, however, that the very tip of the crack reflects the UT beam well, although measurements using the calibration notches suggest that areas extremely close to the tip do indeed reflect the beam. However, there may still be some small regions where, because of the step-like structure of the crack, the signal level drops below the trigger threshold of the electronics. The computer printout in Figure 21 shows this as a singular drop, not to be confused with the "faceting" of the crack surface demonstrated in Figure 20. Conversely, a single inclusion of sufficient size gives an apparent deep crack indication.

Frequently, the crack profile varied during the test in discrete steps. The axial density of scanning, viz. 6 mm (1/4") or 3 mm (1/8"), gave a good statistical image of the crack depth and its profile (Figure 19). The specified accuracy of 0.5 mm was achieved with the help of a calibration notch on each pipe section. In the case of double cracks, as in Figure 16, the computer software recorded only the depth of the deeper one. The CRT operator can recognize the double crack, however, by the changes in the A-scan signal.

Overall, the system performed very well. The real time display of results on the screen permits immediate remedial action when difficulties (such as the shortage of coupling fluid) arise. No noticeable influence of pressure in the pipe section on UT signals was observed.

4.2 COMPARISON OF MEASURED & PREDICTED FATIGUE LIVES

The monitored fatigue lives showed consistently that the predicted lives were longer (Table II and Appendix C). During growth, the facetting of the cracks resulted in considerable ripple and deviation from the ideal shape of the crack (see Figure 9). Also noticeable is the slightly asymmetrical shape of the cracks, caused by faster growth at the deeper end. Asymmetry was also found in the rate of lateral growth. Both the leaks in

tests no. 1 and 2 exhibit this phenomenon, although lateral growth appears to have been slower than vertical growth in the cracks studied.

The temperature dependence of the effect of H_2S was not known. Laboratory experiments at CANMET-EMR have shown the acceleration of growth in the presence of H_2S [1,2]. In our experiments the level was maintained at 100 ppm 50. The higher average H_2S concentration (150 ppm) was measured for test No. 2, which took 1009 blocks to failure. Whether the H_2S induced corrosion rate during this accelerated test is equivalent to any field conditions is difficult to determine.

The scatter in the crack growth can be influenced by the location of the test notch. If the notch is away from the weld toe, as is the case in test no. 2, notch # 3, the growth in the plate, as opposed to the growth in HAZ of the weld, applies.

4.3 CRACK INITIATION UNCERTAINTY

It is important to consider the crack initiation process and the variations in the original notch depth. The number of blocks required to initiate the crack from a notch will vary with D_o,

the original notch depth. D_o showed a considerable variation along the length of the notch. Which of the values for D should be taken as correct or effective? A small change in D_o, especially for a shallow notch, results in a large change in the number of blocks (hundreds or even thousands) to failure. See Appendix D for the predicted fatigue lives.

The influence of double cracking on the growth rate is also unknown. The double crack can be expected to slow down the growth rate.

4.4 CRITICAL CRACK LENGTH FOR RUPTURE

The problem of critical flaw length leading to a leak or rupture was resolved satisfactorily. The 5 cm (2") and 10 cm (4") long notches leaked, while the 25 cm (10") long notch ruptured. We had intended to test a 6" long notch, but its growth was surpassed by the shorter but deeper 5 cm (2") notch in test no. 2. Cracks shorter than 10 cm (4") will probably cause a leak, while those longer than 25 cm (10") will lead to rupture. The pipe inspection "pig" should therefore be sensitive enough to detect flaws longer than 10 cm (4"). This experiment also proved that the energy stored in the compressed oil of a short pipe is sufficient to propagate the crack to rupture, if a longer than

critical crack exists.

5. CONCLUSIONS

The corrosion fatigue crack growth lives of three full size pipe tests were determined. Real time ultrasonics was successfully used to monitor the crack sizes during the pressure cycling by a random spectrum representing the pipeline pressure history. The predicted lives, based on small scale laboratory tests with weld-toe cracks, were shown to be longer than those experienced in field tests by a factor of 2-3. Defects shorter than 10 cm (4") led to leaks, while defects of 25 cm (10") caused the rupture of the pipe. Allowable crack depth for different remaining lives of a pipeline will be analyzed in a subsequent report by CANMET-EMR.

6. ACKNOWLEDGEMENTS

Techno Scientific Inc. wishes to acknowledge the help and interest of Interprovincial Pipe Line personnel, namely D.J. Ross, A.G. Faulder, A. Leniak, and M. Romanow from Edmonton, as well as the keen interest and maintenance care of Westover yard personnel, chiefly A.L. McLeod, A. Sheddon and L. Smith.

Discussions with and the guidance of Dr. V. Vosikovsky of CANMET-EMR were most helpful. The contributions of J.M. Irvine, of WIC, and J.D. Wells and J. Cushon, of TSI are also appreciated.

7. REFERENCES

1. Vosikovsky, O., Cooke, R.J., "An Analysis of Crack Extension by Corrosion Fatigue in a Crude Oil Line," Int. J. Pres. Ves. and Piping (6) 113-129, 1978.

2. Vosikovsky, O., "Corrosion Fatigue Life of a Sour Crude Oil Pipeline," Physical Metallurgy Research Laboratories Report, MRP/PMRL 82-7 (OP-J), to be presented at UTC conference in Bergen, Norway, April 1982.

3. "Ultrasonic Monitoring of Crack Extension by Corrosion Fatigue in Oil Pipelines," Proposal No. R-810501 by Techno Scientific Inc., May 1981.

4. Macecek, M., "Precise Measurement of Internal Undercut in Pipeline Girth Welds," pp 291-299, in Proc. of Int. Conf. Pipeline and Energy Plant Piping, Pergamon Press, Toronto, 1980.

5. Leniak, A., Romanov, M., "Cyclic and Burst Pressure Testing Facility," International Pipeline Limited, 1980.

6. Vosikovsky, O., "Pressure History of a Crude Oil Pipeline," CANMET Report MRP/PMRL 80-13 (CF), March, 1980.

TABLE I

List of the defects used
in this work

Test No.	Notch No.	Do(mm) $\pm$ 0.15	L_o(mm) $\pm$ 1.°
I	1**	1.54	50
	2	1.38	100
	3	2.35*	100
	4	1.7	50
II	1	1.05*	50
	2	0.79	150
	3	0.82	150
	4	0.86	50
III	1	2.1*	250
	2	1.3	300

* failure notch

**calibration notches marked as No. 5 in Figure 5 are not listed here.

Do - initial depth of the notch

L_o - initial length of the notch

TABLE II

Crack Growth in Tests No. 1 & No. 3

Test No.	Notch #	Do(mm)	D32(mm)	D56(mm)	D86(mm)	D106(mm)	D Met	R
I	1	1.54	1.6	1.6	1.8	1.9	1.61	1.
	2	1.38	1.5	1.5	1.7	1.7	1.60	4.1
	3*	2.35	2.8	3.1	4.1	7.1	7.1	1.5
	4	1.64	2.0	2.0	2.1	2.8	2.56	3.0
			D32	D52	D82	D Met		
	1**	2.1	2.6	3.2	7.1	7.1		1.4
III	2	1.30	1.3	1.4	1.7	1.54		7.3

Number following maximum crack depth D is the number of applied blocks.
In the last column it indicates No. of blocks to failure.
D-met crack depth measured on cross sections.

R - ratio of predicted number of blocks using the Table A1 in appendix versus the number of blocks which occured. Numbers larger than 1 mark unconservative prediction.

$$R = \frac{Nth.}{Nexp.}$$

* - leak

** - break

Table II (continuation)

Crack growth in pipe No. 2

Notch #	1*	2	3	4
Do(mm)	1.05	0.79	0.82	0.86
D (127)	1.5	0.8	1.0	1.0
D (242)	1.5	0.8	1.0	1.0
D (385)	1.5	0.8	1.0	1.1
D (569)	1.7	1.0	1.1	1.0
D (704)	1.7	1.0	1.5	1.1
D (800)	1.7	1.0	1.8	1.1
D (862)	1.9	1.4	2.0	1.1
D (911)	2.2	1.9	2.1	1.1
D (960)	3.5	2.1	2.6	1.2
D_{UT} (1009)	7.1	3.2	3.4	1.1
D_{met} (1009)	7.1	2.9	3.2	1.1
R	2.81	9	7.1	--

* Leak

List of Figures

Figure 1. Principle of the ultrasonic crack depth measurement method.

Figure 2. Block diagram of the testing system including computer interfacing.

Figure 3. Overall view of the experimental testing facility for fatigue crack growth monitoring.

Figure 4. Close-up of the ultrasonic scanner mounted on the pressure vessel.

Figure 5. Typical location of test notches on the pressure vessel (see also Table I).

Figure 6. Notch profiles for pipe #2, notch no. 2 at A-0, B-700, C-862, D-960 and E-1009 blocks.

Figure 7. Dependence of maximum crack depth on number of blocks for tests no. 1 and 3.

Figure 8. Dependence of maximum crack depth on number of blocks for test no. 2.

Figure 9. Freeze-break fracture faces in tests no. 1 and 2.

Figure 10. Oil jet rising from leak in pressure vessel.

Figure 11. Appearance of pressure vessel after rupture in test no. 3.

Figure 12. Cut-out section of ruptured pipe showing deviation of crack away from weld.

Figure 13. Fractography of test no. 3 showing original notch, fatigue growth of crack, and ductile fracture of the parent plate.

Figure 14. Typical cracks developed during corrosion fatigue tests.

Figure 15. Higher magnification micrograph showing crack geometry and tightness of crack tip.

Figure 16. Development of double cracks in notches with sharp corners.

Figure 17. Crack initiation after 106 blocks in test no. 1. Notch location simulates true weld toe crack.

Figure 18. Different position of test notch with respect to root of weld caused by weld wander in test no. 2.

Figure 19. An example of a computer printout showing the depth profile of a short notch.

Figure 20. An example of a computer printout showing the facetted growth of a crack in test no. 2.

Figure 21. Computer printout showing through the wall defect (leak) in test no. 2.

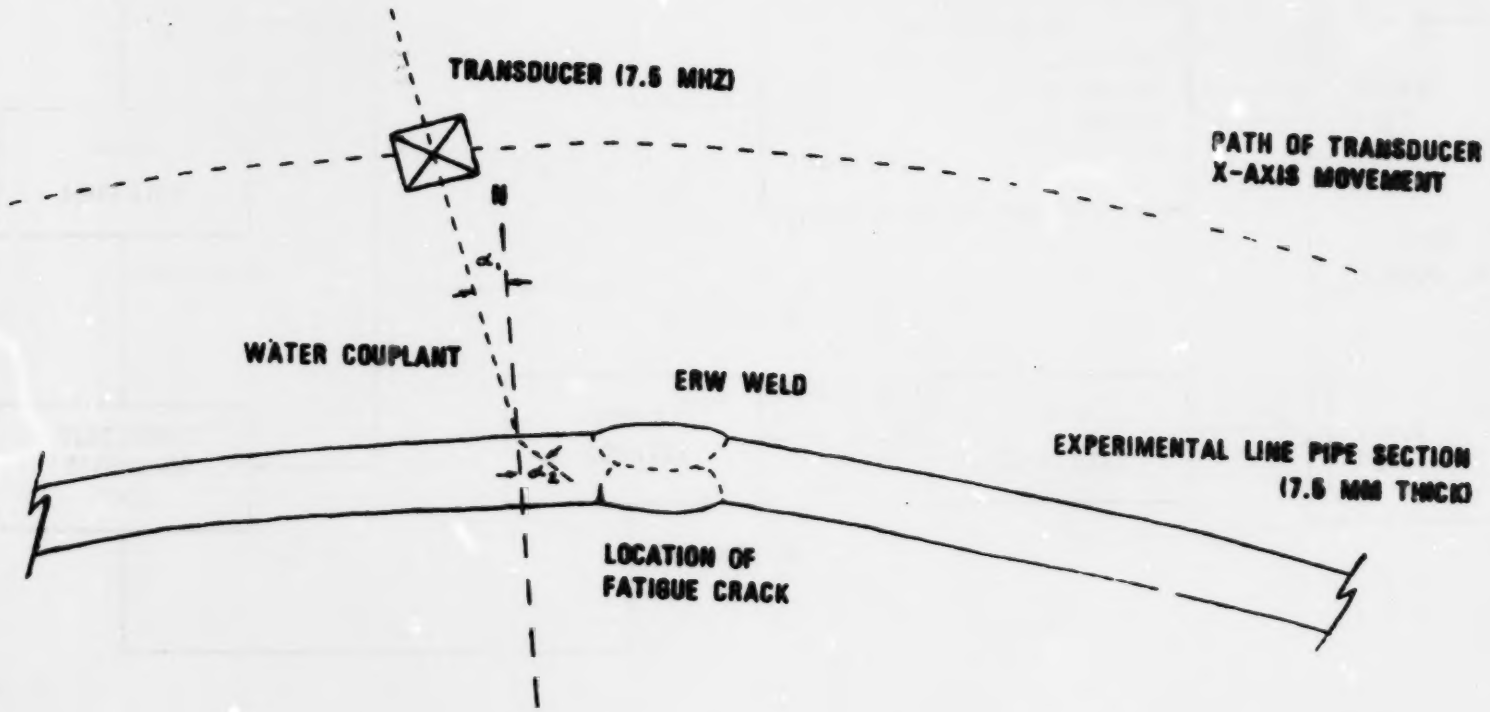

Figure 1 Principle of the ultrasonic crack depth measurement method.

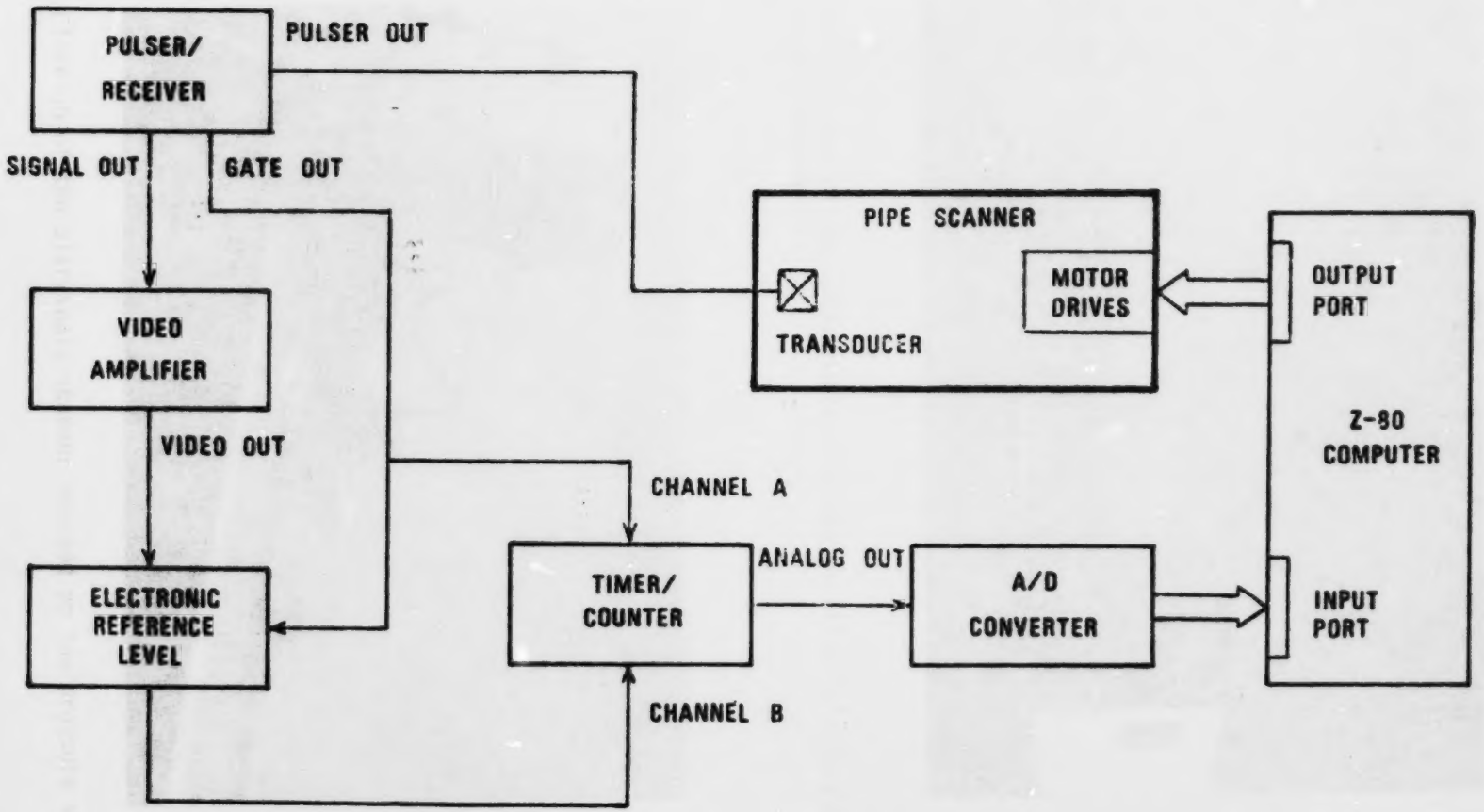

Figure 2 Block diagram of the testing system, including computer interfacing.

Figure 3 Overall view of the experimental testing facility for fatigue crack growth monitoring.

Figure 4 Close-up of the ultrasonic scanner mounted on the pressure vessel.

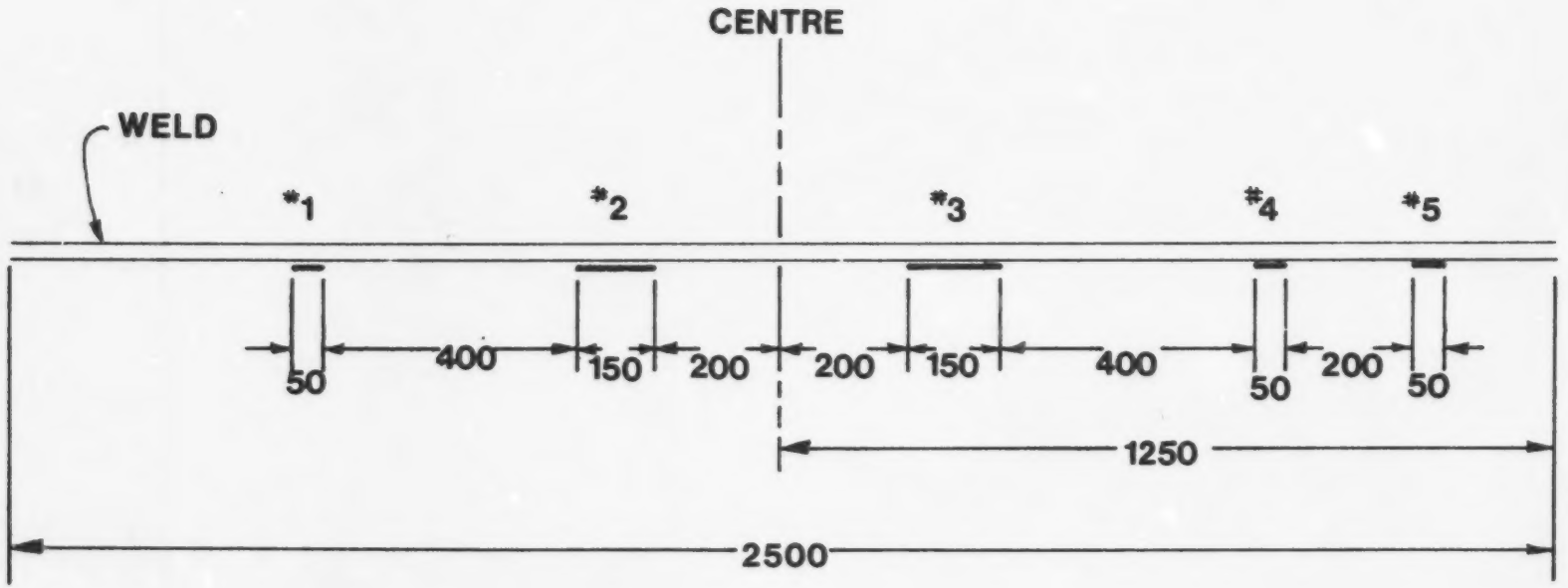

Dimensions in mm

Figure 5 Location of test notches on test section #2 (see also Table I). #5 is the calibration notch

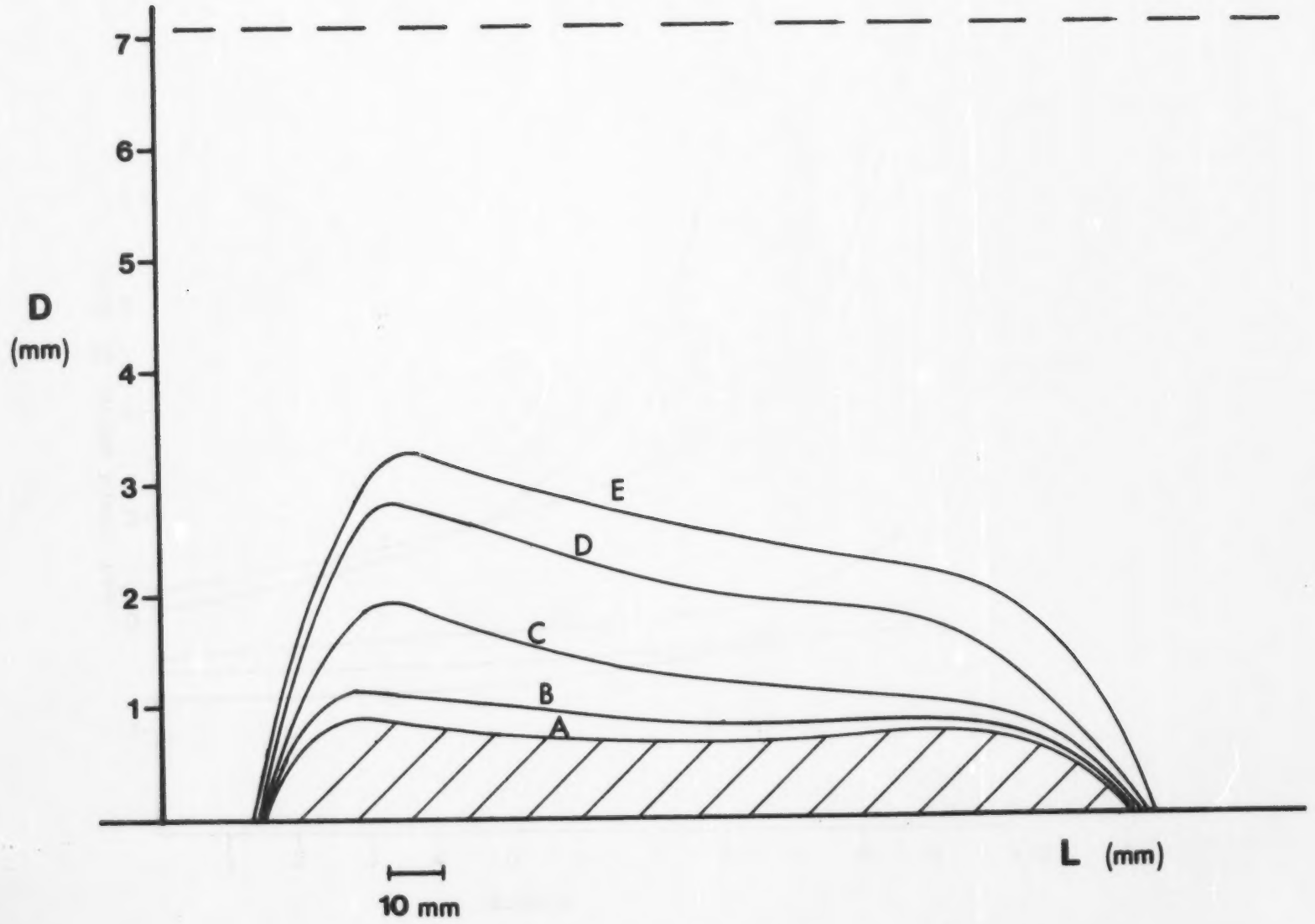

Figure 6 Notch profiles for pipe #2, notch no. 2 at A-0, B-700, C-862, D-960 and E-1009 blocks.

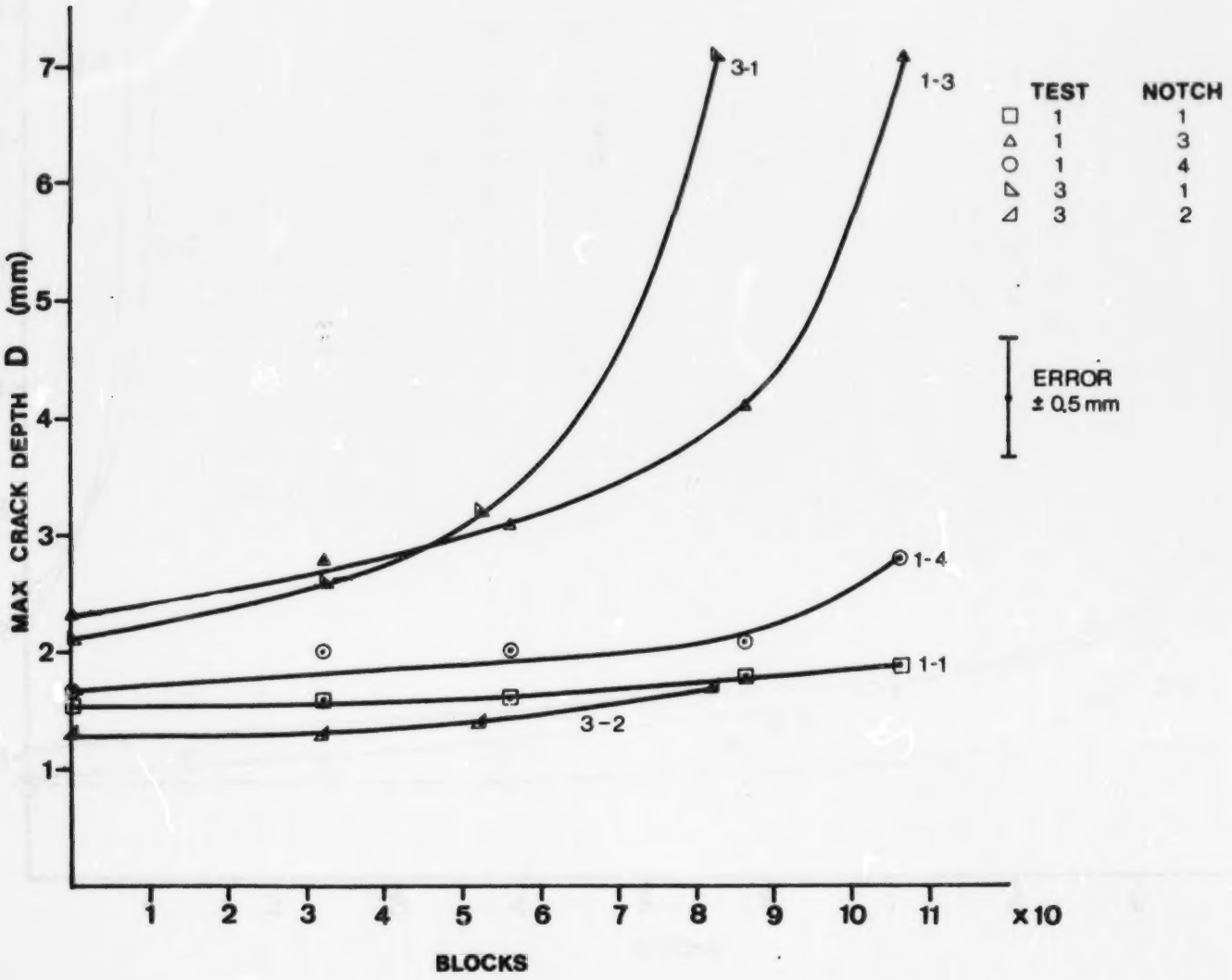

Figure 7 Dependence of maximum crack depth on number of blocks for tests no. 1 and 3.

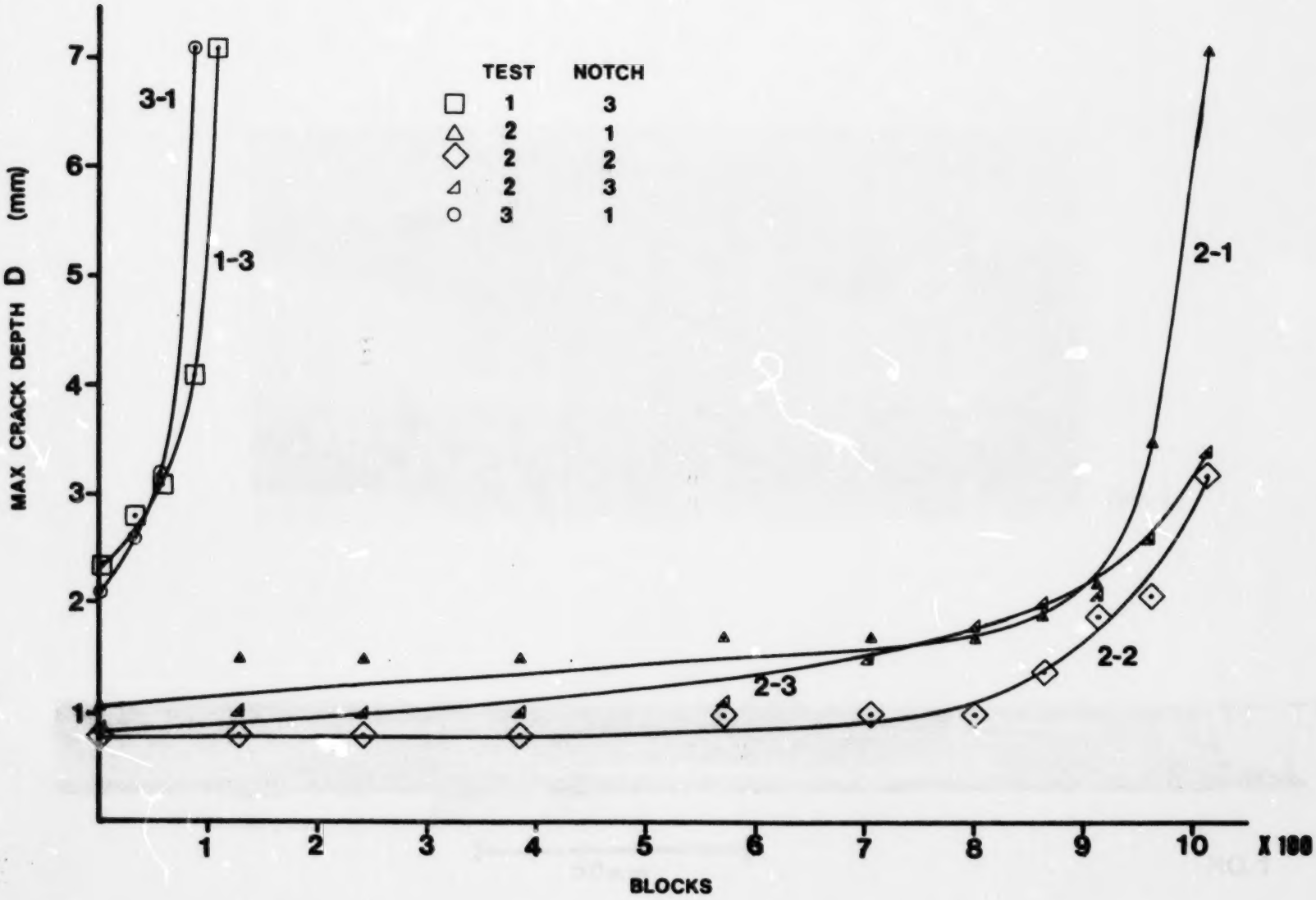

Figure 8 Dependence of maximum crack depth on number of blocks for test no. 2.

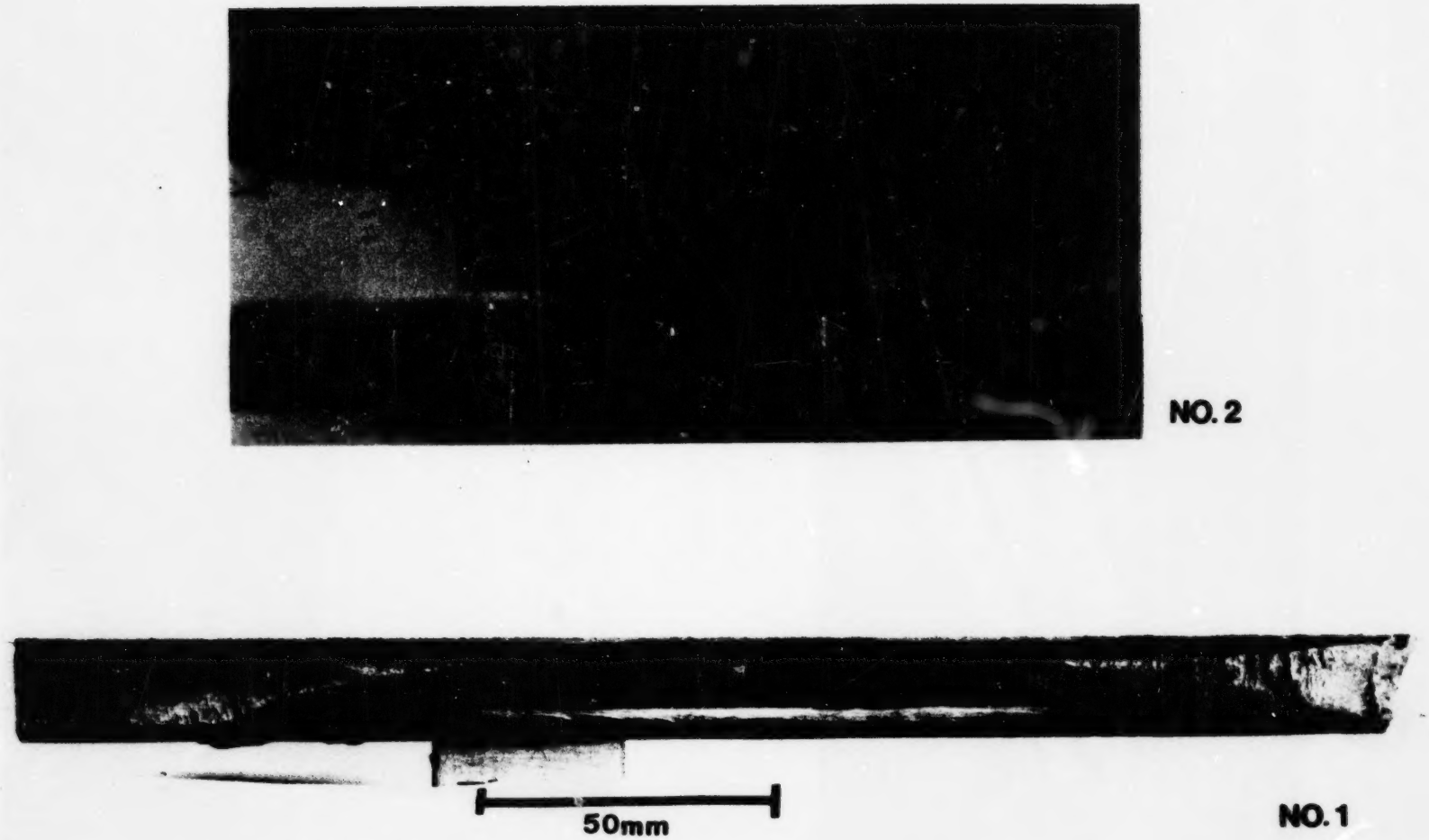

Figure 9 Freeze-break fracture faces in tests no. 1 and 2.

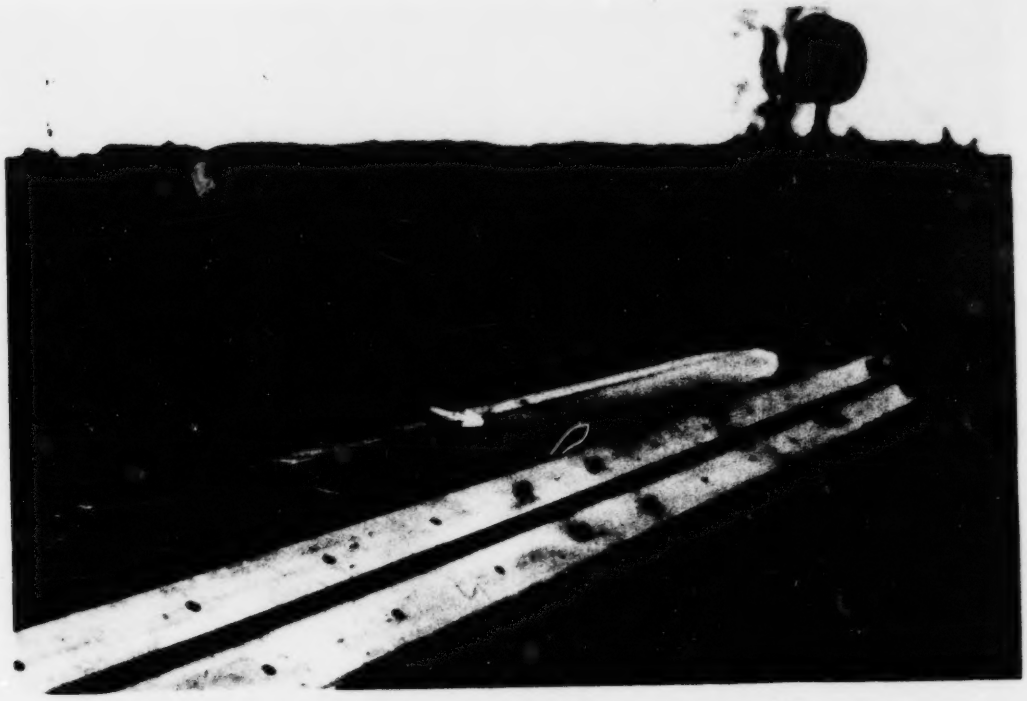

Figure 10 Oil jet rising from leak in pipe section.

Figure 11 Appearance of pipe section after rupture in test no. 3.

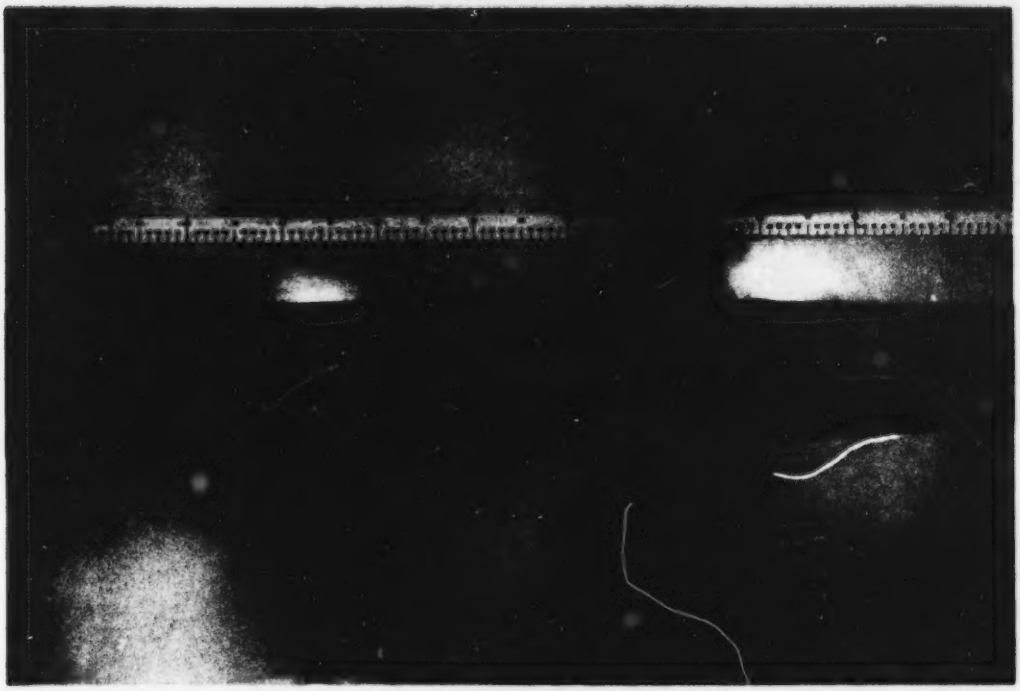

Figure 12 Cut-out section of ruptured pipe showing deviation of crack away from weld.

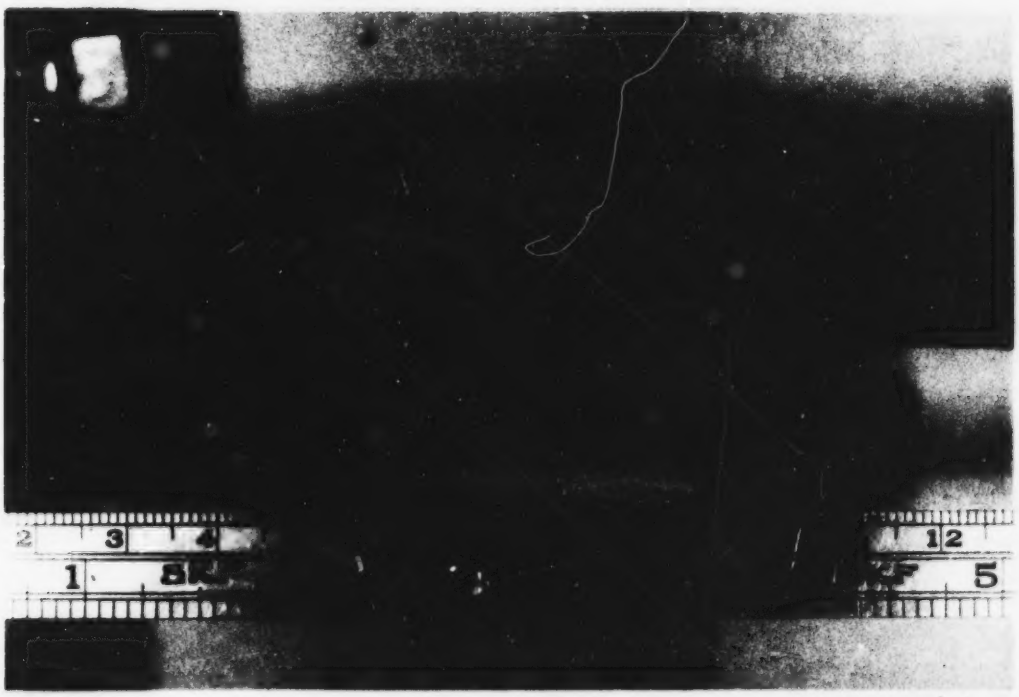

Figure 13 Fractography of test no. 3 showing original notch, fatigue growth of crack, and ductile fracture of the parent plate.

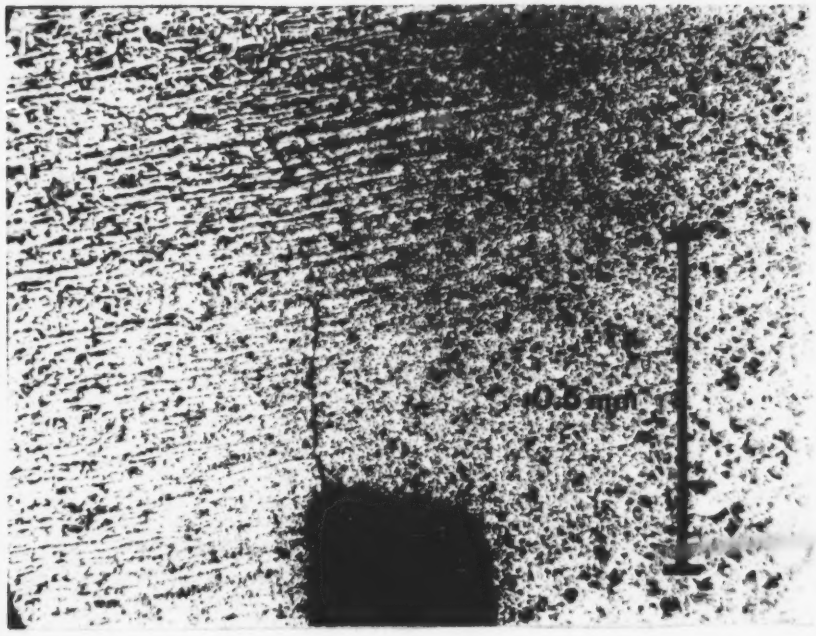

TEST 3
NOTCH 2

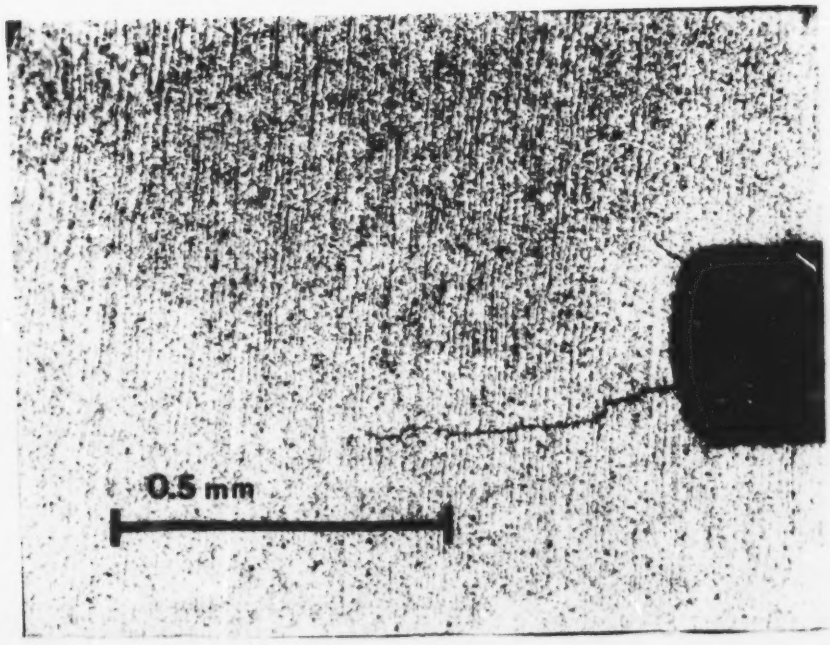

TEST 1
NOTCH 2

Figure 14 Typical cracks developed during corrosion fatigue tests.

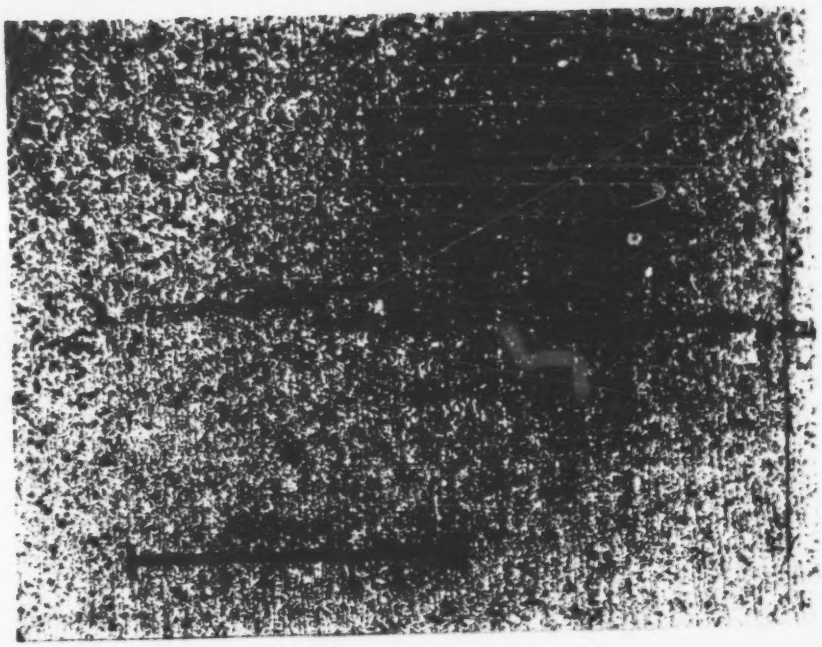

TEST 2
NOTCH 4

Figure 15 Higher magnification micrograph showing crack geometry and tightness of crack tip.

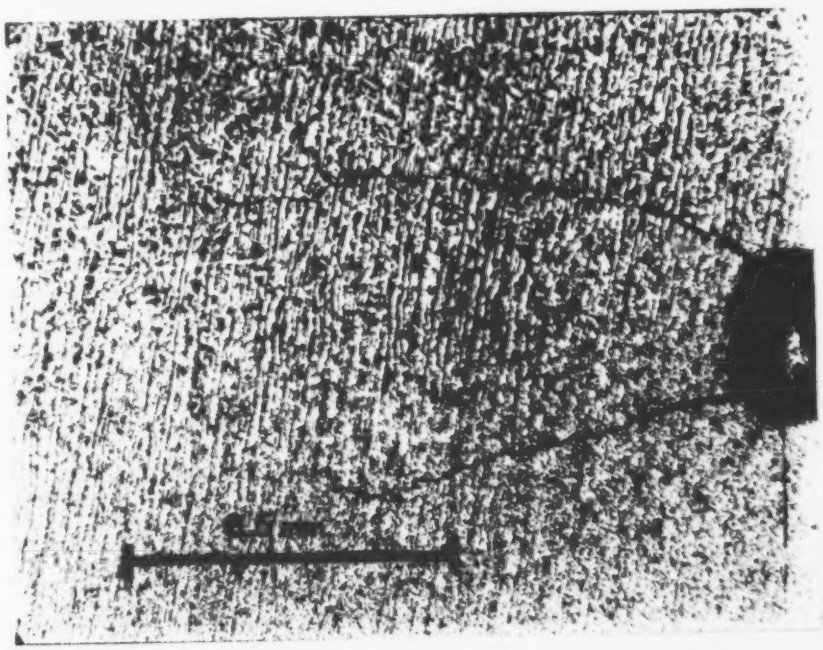

TEST 1
NOTCH 4

Figure 16 Development of double cracks in notches with sharp corners.

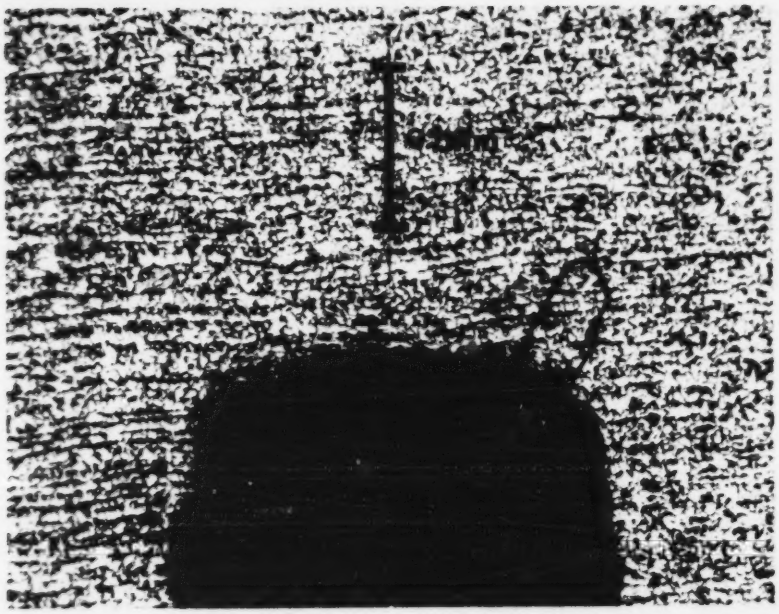

TEST 1
NOTCH 1

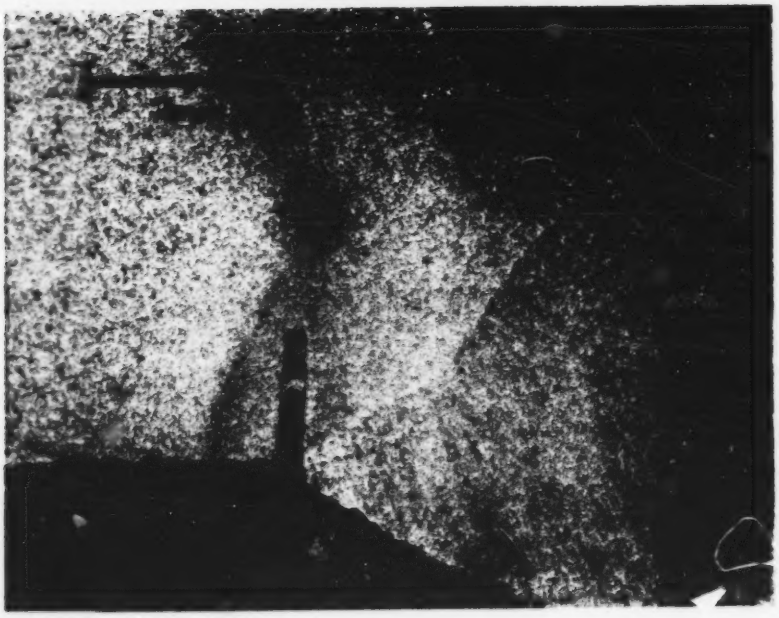

TEST 1
NOTCH 1

Figure 17 Crack initiation after 106 blocks in test no. 1. Notch location simulates true weld toe crack.

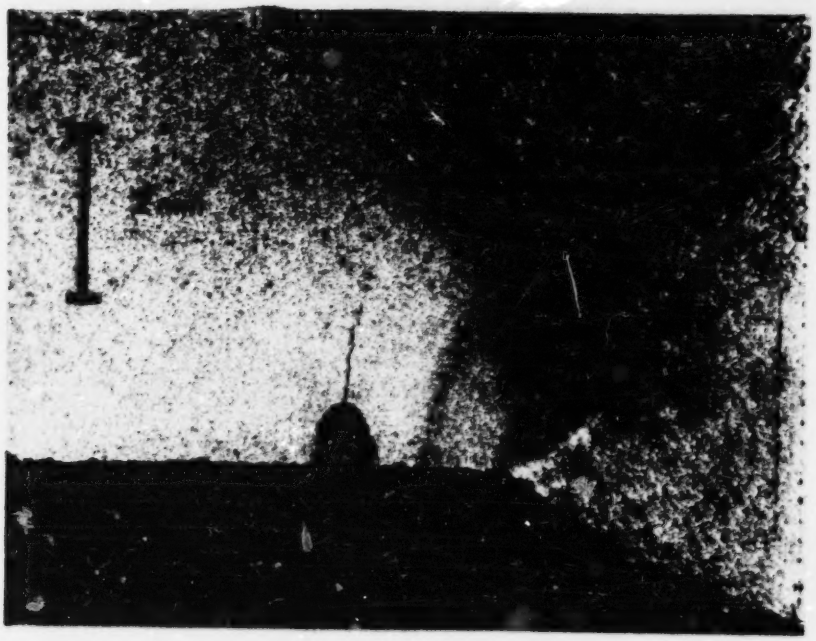

TEST 2
NOTCH 2

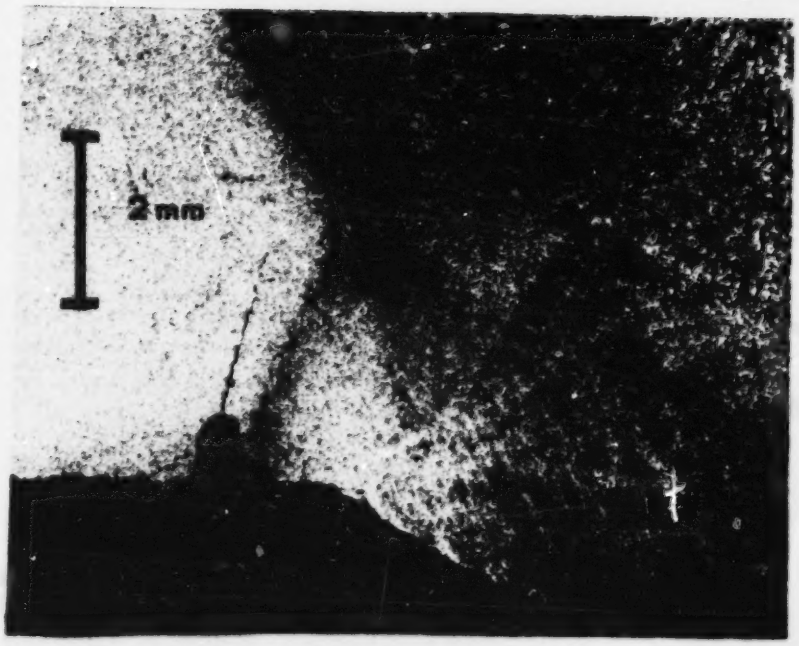

TEST 2
NOTCH 2

Figure 18 Different position of test notch with respect to root of weld caused by weld wander in test no. 2.

D_R, R Maximum crack depth measured during scan approaching the weld.

D_L, L Maximum crack depth measured during scan leaving the weld.

AXIAL STEP 0.125"

AXIAL POSITION	D_R	D_L	
000.89	0.0006	0.0006	*
000.90	0.0013	0.0006	LR
000.92	0.0026	0.0006	L R
000.93	0.0013	0.0006	LR
000.94	0.0006	0.0118	R L
000.96	0.0099	0.0066	L R
000.97	0.0099	0.0105	RL
000.98	0.0099	0.0132	R L
001.00	0.0105	0.0118	RL
001.02	0.0105	0.0130	R L
001.11	0.0132	0.0151	R L
001.13	0.0105	0.0125	R L
001.15	0.0118	0.0144	R L
001.18	0.0118	0.0125	L R
001.20	0.0105	0.0125	R L
001.22	0.0118	0.0138	R L
001.10	0.0105	0.0105	*
001.12	0.0112	0.0131	R L
001.15	0.0132	0.0150	R L
001.14	0.0112	0.0092	L R
001.16	0.0085	0.0013	L R
001.17	0.0006	0.0013	RL
001.18	0.0066	0.0006	L R
001.20	0.0006	0.0006	*
001.21	0.0006	0.0006	*
001.22	0.0006	0.0006	*
001.24	0.0006	0.0006	*

1 mm — CRACK DEPTH

Figure 19 An example of a computer printout showing the depth profile of a short semi-elliptical notch.

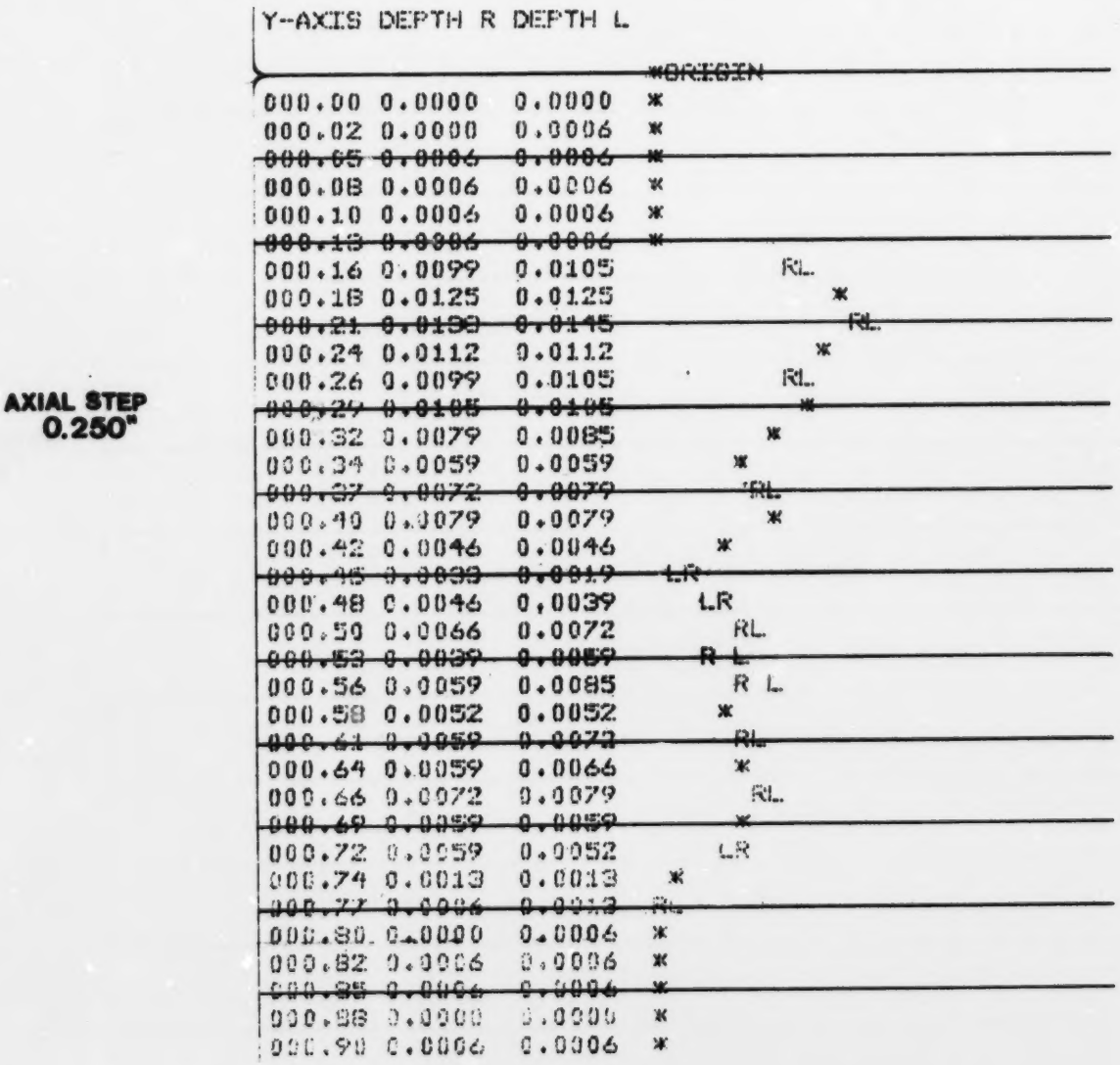

AXIAL STEP 0.250"

Figure 20 An example of a computer printout showing the facetted growth of a crack in test no. 2.

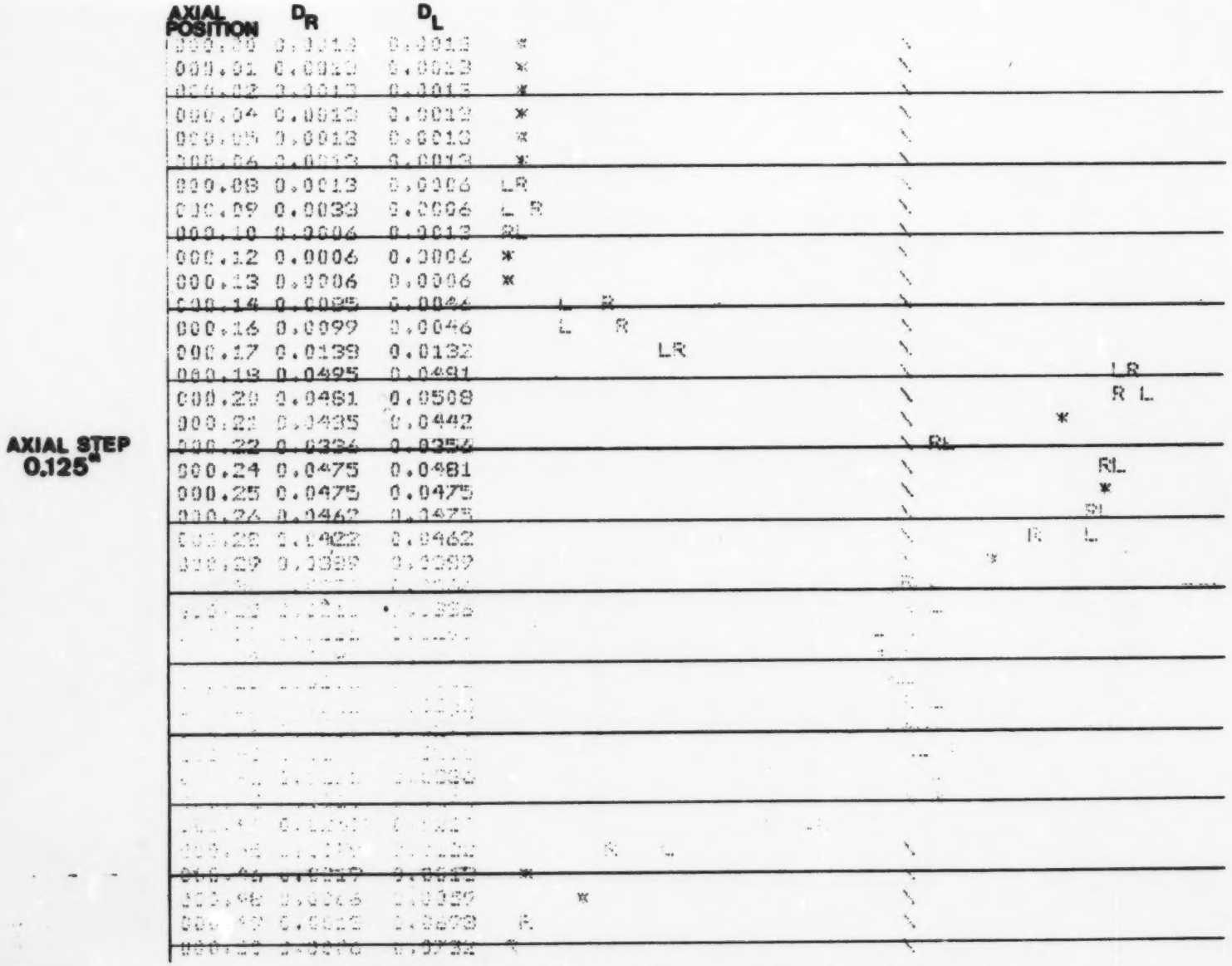

Figure 21 Computer printout showing through the wall defect (leak) in test no. 2.

Appendix A

H_2S concentration in crude oil for test I, II and III

Test No.	H_2S concentration (ppm)*			
I	79	(35) 69		
II	(24) 199	(300) 150	(600) 120	
III	(24) 127			

* The number in brackets marks the number of blocks at which the sample was taken.

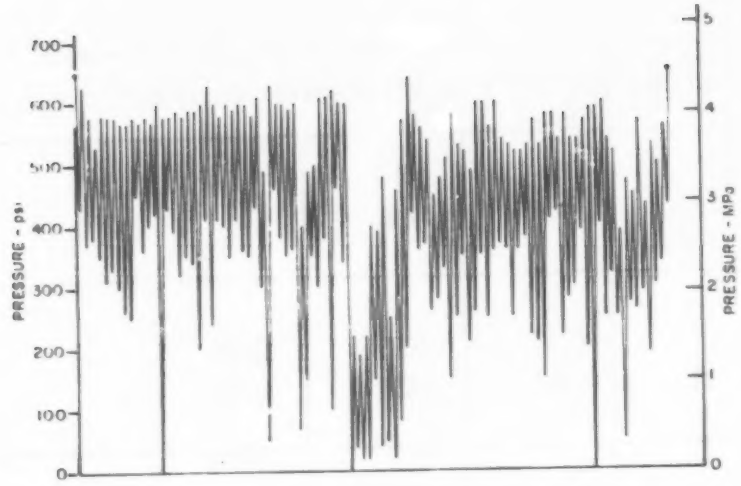

Appendix B: Pressure spectrum during one test block.

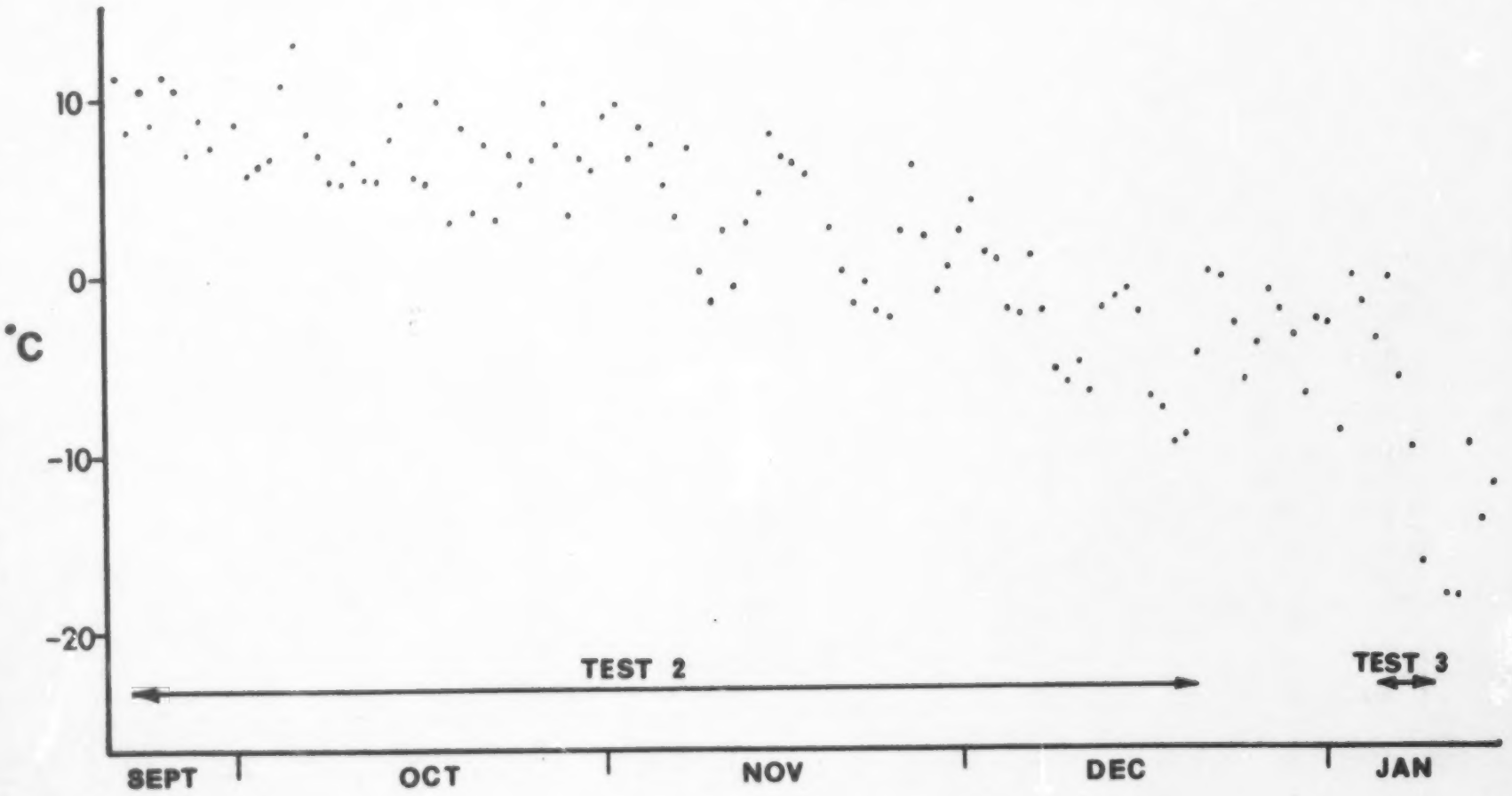

Appendix C: Temperature variations during tests. For test #1, the average temperature was higher than 14 degrees. For test #3, the oil temperature was 8-10°C above the air, because of the enclosure. Temperature Data are for Toronto International Airport about 10 km away from the test site.

FATIGUE LIFE PREDICTION

BLOCKS PROCESSED SINCE START	NO. OF BLOCKS PROCESSED SINCE LAST PRINT LINE OR START	CHANGE IN CRACK SIZE CAUSED BY LAST BLOCK	CHANGE IN CRACK SIZE SINCE LAST PRINT LINE OR START	CURRENT SIZE OF CRACK	KMAX
1	1	.000017	.000017	.700017	.150E+02
4500	4499	.000029	.100016	.800034	.163E+02
7176	2676	.000048	.100032	.900066	.176E+02
8845	1669	.000076	.100021	1.000087	.190E+02
9915	1070	.000117	.100002	1.100089	.203E+02
10618	703	.000176	.100139	1.200228	.217E+02
11087	469	.000261	.100058	1.300286	.231E+02
11406	319	.000381	.100161	1.400448	.245E+02
11626	220	.000550	.100283	1.500731	.260E+02
11779	153	.000787	.100333	1.601064	.276E+02
11887	108	.001119	.101040	1.702104	.292E+02
11963	76	.001579	.100802	1.802906	.308E+02
12017	54	.002217	.100910	1.903816	.326E+02
12056	39	.003082	.102418	2.006234	.344E+02
12085	29	.003873	.100511	2.107045	.363E+02
12109	24	.004862	.104726	2.211771	.383E+02
12128	19	.005916	.102648	2.314419	.405E+02
12144	16	.007156	.104606	2.419045	.428E+02
12157	13	.008684	.103074	2.522118	.451E+02
12168	11	.010594	.104355	2.626474	.477E+02
12177	9	.012734	.105120	2.733594	.504E+02
12185	8	.015710	.114482	2.848076	.536E+02
12191	6	.018738	.104359	2.952435	.567E+02
12196	5	.022173	.103547	3.055982	.599E+02
12201	5	.027084	.124656	3.180638	.641E+02
12205	4	.032422	.121190	3.301828	.684E+02
12208	3	.038291	.108493	3.410321	.726E+02
12211	3	.046844	.130525	3.541146	.788E+02
12213	2	.054252	.104422	3.645568	.827E+02
12215	2	.062288	.123231	3.768799	.885E+02
12217	2	.071484	.147887	3.916687	.962E+02
12218	1	.080278	.080278	4.082877	.101E+03

** LAST BLOCK **
** END OF RUN **

Appendix D: Fatigue Life Prediction, based on growth rate of weld toe defect. Crude oil with 100 ppm of H_2S.

POOR

QUALITY

ORIGINAL